Refuse derived bio-organics and immobilized soybean peroxidase for green chemical technology

(Article begins on next page)

24 April 2024

This is an author version of the contribution published on:

The definitive version is available at:

1 Refuse derived bio-organics and immobilized soybean peroxidase

2 for green chemical technology

3 Giuliana Magnacca,[a,*] Enzo Laurenti,[a] Erika Vigna,[a] Flavia Franzoso,[a]

4 Lorenzo Tomasso,[a] Enzo Montoneri,[a] and Vittorio Boffa[b]

5

6 *Dipartimento di Chimica, NIS Centre of Excellence, Universitá di Torino, Via

7 P.Giuria 7, I-10125 Torino, Italy, Fax: +39 011 670 7855; Tel: +39 011 670

8 7543; e-mail: *giuliana.magnacca@unito.it*

9 [a] Dipartimento di Chimica, Universitá di Torino, Via P.Giuria 7, I-10125 Torino,

10 Italy; *enzo.laurenti@unito.it*; *enzo.montoneri@unito.it*

11 [b] Section of Chemistry, Aalborg University, Shongårdsholmsvej 57, 9000 DK

12 Aalborg, Denmark, *vb@bio.aau.dk*

13

14

Abstract

A silica monolith was prepared from commercial silica powder dispersed in water containing polymeric water soluble bio-organics (SBO) isolated from composted urban vegetable wastes. The monolith and the pristine powder were characterized for their morphology and reactivity for immobilizing Soybean Peroxidase (SBP). Compared to the pristine powder, the monolith exhibited lower specific surface area (about 30% less), total pore volume and pore size (of about 200 Å of width), and bond less SBP under the same experimental conditions. The immobilized SBP products were tested for their catalytic activity in the reaction of hydrogen peroxide, 3-(dimethylamino)benzoic acid (DMAB) and 3-methyl-2-benzothiazolinone hydrazone (MBTH), by comparison with the same reaction performed with native SBP in solution. The reaction performed in the presence of immobilized SBP was slower than that catalyzed by native SBP in solution. However, in spite of its lower SBP content, monolith immobilized SBP (M-SBP) was found kinetically more active than the powder immobilized SBP (P-SBP). Also, M-SBP allowed to achieve the same reagents conversion as native SBP (95% of reagent conversion), although in longer time, whereas the maximum reagent conversion achieved with P-SBP was much lower (75% of reagent conversion). The M-SBP was more easily recovered from the reaction medium and found more stable than P-SBP upon repeated catalyst recycling (after 20 cycles 75-80% of the initial activity was retained by both immobilized samples, slightly higher in the case of M-SBP).

38   Biocatalysis, Biomass, Monolith preparation, Oxidoreductasis, Porous material

39

40

Introduction

Developing new immobilized biocatalysts is a current trend in green chemistry to perform reactions in heterogeneous media rather than in homogeneous media where the catalyst recovery is economically and environmentally critical. Also, valorization of biowastes as source of chemicals is a mean to cope with increasing amount of wastes. Within these scopes, the present work exemplifies urban refuse as sustainable renewable resource for the development of cost effective innovative technology to establish new, greener and safer chemical processes.

Previous work has indeed demonstrated the potential of urban bio-wastes (UBW) to be a cost-effective exploitable source of soluble bioorganics (SBO) to recycle to the chemical and consumer's market.[1] Indeed, as result of increased production due to population urbanization, UBW are concentrated in confined areas by municipal collection. Also, they are a rather rich source of bio-organic matter. This, depending on the source nature and waste management process conditions, may run up to 40–60% concentration and, in principle, provides a wide variety of products fitting a number of diversified specific technological requirements and consumer's needs.

The above SBO are described as mixtures of macromolecules with average molecular weight (Mw) values ranging from 67 to 463 kg mol^{-1} and number average molecular weight (Mn) yielding polydispersity index values (Mw/Mn) in the 6 to 53 range. Chemical composition data also show that these macromolecules contain several functional groups and C types of different polarity. They appear to be formed by long aliphatic C chains substitued by

65   aromatic rings and several functional groups as COOH, CON, C=O, PhOH, O-

66   alkyl, OAr, OCO, OMe, and NRR', with R and R' being alkyl C or H as

67   represented in the molecular fragment shown in Figure 1. Although entirely

68   virtual, this molecular fragment helps to memorize analytical chemical data and

69   to expect chemical-physical properties. Indeed, consistently with Figure 1

70   representations, SBO have been found to exhibit typical properties of anionic

71   surfactants and polyelectrolites.[2] In essence, they are capable to lower the

72   surface tension of water and to change their molecular conformation in solution

73   or yield macromolecular aggregates with 100-300 nm or larger hydrodynamic

74   diameter as a function of concentration. The solution behavior of SBO has

75   allowed their use as templates for fabricating mesoporous silica powders by sol-

76   gel reaction[3] starting from tetraethylorthosilicate (TEOS) and 3-

77   aminopropyltriethoxysilane (APTES). On the other hand, by the presence of the

78   above polar functional groups, SBO have been reported capable to interact with

79   inorganic oxides and perform as dispersants or flocculants of these materials

80   depending on the experimental conditions.[1] These results have offered the

81   scope for testing further the potential of SBO in the field of catalysts

82   preparations.

83   The present work was undertaken with two specific aims: (i) to find out if the

84   same previously reported silica material could be obtained in presence of SBO

85   by an alternative procedure not involving the use of silane reagents and organic

86   solvent (see, for instance,ref. 4), and (ii) to test the silica product in

87   heterogeneous biocatalysis.

88   To this purpose a commercial silica (obtained by precipitation in aqueous

89   medium) was dispersed in water in the presence of SBO derived from

composted urban vegetable residues, dried and heated to 500°C to yield a

mesoporous monolith. This material was used as support to immobilize

Soybean Peroxidase (SBP).

The reaction of hydrogen peroxide, 3-(dimethylamino)benzoic acid (DMAB) and

3-methyl-2-benzothiazolinone hydrazone (MBTH), catalyzed by Soybean

Peroxidase (SBP) was chosen to evaluate the performance of the immobilized

catalyst versus the free catalyst dissolved in a homogeneous reaction medium.

The choice of SBP as active probe in this work is due to the ability of this

enzyme to catalyze the oxidation of a large number of organic and inorganic

substrates by means of hydrogen peroxide,[5,6] and its high resistance to thermal

and chemical denaturation.[7,8] This makes SBP very interesting for

biotechnological applications, in particular when the immobilization on solid

support is requested in order to favor the removal of the enzyme from the

reaction bath and its reuse for many reaction cycles. The hereinafter reported

results will show the importance of the morphological changes induced in silica

prepared in the presence of SBO for the immobilized SBP stability and

performance.

Experimental

Materials

The SBO in 10% w/w yield was obtained from park home gardening residues

and public park trimmings composted for 230 days at the Acea Pinerolese plant

in Pinerolo, Torino, Italy. According to a previously reported procedure,[1] the

composted material was further processed in a pilot plant made available by

Studio Chiono e Associati in Rivarolo Canavese, Italy. This comprises an

electrically heated mechanically stirred 500 L reactor, a 102 cm long x 10.1 cm

diameter (7.9 m^2 of surface) polysulfone ultrafiltration (UF) membrane with 5 kD

molecular weight cut-off supplied by Idea Engineering s.r.l. from Lessona (Bi),

Italy, and a forced ventilation drying oven. According to the operating

experimental conditions, the compost was reacted 4 h with pH 13 water at 60

°C and 4 L/kg water/solid ratio. The liquid/solid mix was allowed to settle to

separate the surnatant liquid phase containing the soluble compost hydrolyzate

from the insoluble residue. The recovered liquid phase was circulated at 40 L h^{-1}

flow rate through the UF membrane operating with tangential flow at 7 bar inlet

and 4.5 bar outlet pressure to yield a retentate with 5-10 % dry matter content.

The concentrated retentate was finally dried at 60 °C. The final product obtained

in 15 % w/w yield, relatively to the starting compost dry matter, was isolated as

a black solid with dry matter containing 38.25 % w/w carbon, 4.01 % w/w

nitrogen and 27.1 % w/w ashes. It was further characterized by ^{13}C NMR and

potentiometric titration, and by surface tension measurements, according to a

previously reported[1] analytical protocol.

The silica powder (FK320) was purchased from Degussa. This product is

claimed by the vendor to be obtained by precipitation from sodium silicate in

water acidified with sulphuric acid. Soybean peroxidase (SBP, EC 1.11.1.7) RZ

=2.0 was purchased from Bioresearch Products Inc. (Iowa, USA) and used

without further purification. Hydrogen peroxide 30%, 3-(dimethylamino)benzoic

acid (DMAB) and 3-methyl-2-benzothiazolinone hydrazone (MBTH) were

purchased from Sigma-Aldrich Italia.

Monolith preparation

SBO (1 g) was kept under stirring in 15 ml water for 2 hours. Silica particles (4 g) were added to the black SBO solutions. More water (10 ml) was then added to favor mixing of the reagents under stirring for two hours. The system showed thixotropic behavior, and vigorous stirring favored the formation of a fluid phase with low viscosity. After relaxing for two hours, the mixture became thicker to yield finally a black wet pellet with the shape of the container in which the preparation was carried out. This material was let drying at room temperature for three days, removed afterwards from the container and calcined in oven at 500°C for four hours in order to remove all organics and yield a porous monolith.

Immobilization of SBP on silica

One gram of pristine silica powder or monolith was suspended in 0.075 L of a 10% v/v solution of 3-aminopropyltriethoxysilane in water. The pH was adjusted to 4.0 with HCl and the mixture was heated at 80°C for three hours in a water bath. The resulting suspension was filtered on a buchner funnel and the product was washed with bidistilled water and dried at 120°C. Successively, 0.5 g of silanized product were suspended in 0.050 L of glutaraldehyde 2.5% v/v in 0.1 M phosphate buffer solution at pH 7.0, and allowed to react for 1 h in the dark at room temperature. The resulting suspension was then filtered. The recovered solid was washed four times, added to 0.005 L of 2.5 mg mL^{-1} soybean peroxidase solution in 0.1 M phosphate buffer at pH 7.5 and left to react at 4°C for 20 h. The final product, obtained by filtration, washing four times with the same buffer and gentle drying, was stored at 4ºC. The amount of SBP

164 immobilized was calculated as the difference between the initial amount of

165 enzyme and that recovered in the washing liquid. The concentration of SBP in

166 solution was determined by means of UV-Visible spectroscopy, measuring the

167 absorbance at 403 nm as previously reported[9].

168

169 *Materials characterization methods*

170 N_2 gas-volumetric adsorption at 77 K (ASAP2020 by Micromeritics) for the

171 determination of specific surface area (BET model)[10] and porosity (BJH

172 model)[11] were performed according to the cited literature on powder and

173 monolith samples activated in vacuum (residual pressure 10^{-2} mbar) at 60°C

174 prior to analysis.

175 High-Resolution Transmission Electron Microscopy was performed on a JEOL

176 JEM 3010UHR (300 kV) TEM fitted with a single crystal LaB_6 filament. All

177 samples were dry deposited on Cu "holey" carbon grids (200 mesh).

178

179 *Kinetic measurements*

180 The catalytic properties of immobilized SBP materials were tested by using the

181 DMAB-MBTH reaction[12]. Before to start the kinetic measurements, silica

182 powder and monolith were incubated for 1 h in acetate buffer 0.1 M pH 5.4.

183 Then, 6 mg of immobilized SBP samples (on powder and monolith, indicated as

184 P-SBP and M-SBP, respectively), or 10 μL of SBP in solution, were placed in a

185 reactor (pyrex beaker) together with 6 mL of a solution of the same buffer

186 containing 3-(dimethylamino)benzoic acid (DMAB) $5.0^{.}10^{-4}$ M and 3-methyl-2-

187 benzothiazolinone hydrazone (MBTH) $2.1^{.}10^{-5}$ M. The SBP amounts were:

188    $2.5 \cdot 10^{-9}$ mol on P-SBP, $1.8 \cdot 10^{-9}$ mol on M-SBP, and $8.3 \cdot 10^{-11}$ mol for the free

189   protein, respectively.

190   The reaction was started by adding hydrogen peroxide $6.4 \cdot 10^{-5}$ M. During the

191   tests, the reaction mixture was continuosly stirred and maintained at 25 °C..

192   The reaction was followed by recording the absorbance at 590 nm ($\varepsilon_{590\ nm}$ =

193   47600 $M^{-1}cm^{-1}$) at different reaction times for 4 hours. For each test-time, the

194   stirring was stopped for about one minute, ~3 ml of supernatant was transferred

195   in a quartz cuvette for spectroscopic analysis and afterwards put back in the

196   reactor.

197   In the case of free-enzyme experiments, ~3 ml of the solution were analyzed

198   without separating SBP from substrate. In no cases, SBP signals interferred

199   with 590 nm band.

200   The conversion rates were calculated with respect to the stoichiometric amount

201   of the DMAB-MBTH product that can be obtained in these experimental

202   conditions.

203

204   **_Results_**

205   _Chemical and physico-chemical characterization of SBO_

206   The SBO material used in this work is a product of biological origin. It is sourced

207   from urban private yard residues and public park trimmings which have

208   undergone aerobic biodegradation for 230 days. It has quite complex chemical

209   composition. Assessment of its chemical nature is rather difficult, owing to the

210   broad distribution of molecular weight and to the content of many organic

211   moieties from the main constituents of vegetable matter which are not

212 completely mineralized by biodegradation. At best, it may be characterized for

213 its content of organic matter obtained from the weight loss after calcination at

214 650°C, its C and N elemental analytical data, and its organic moieties and

215 functional groups content obtained by ^{13}C NMR spectroscopy as reported in

216 Table 1. Organic matter in SBO can be virtually represented by molecular

217 fragments such as that shown in Figure 1, where aliphatic and aromatic C

218 moieties and functional groups fit analytical data. Besides the organic content,

219 SBO exhibits some minor inorganic components which are reported and

220 quantified in Table 2.

221   Water surface tension (γ) vs. SBO concentration (Cs) data, such as those

222 reported in Fig. 2, are a useful tool to understand the behavior of the above

223 SBO in solution and suggest potential uses for it. The experimental data show a

224 clear trend of γ to decrease upon increasing Cs. This feature has been

225 reported for other similar substances isolated from different urban biowastes.[2]

226 The observed slope changes in the γ-Cs plots have been explained to arise

227 from conformational changes occurring for the polymeric substances in

228 aqueous solution. These are capable to assume coil conformation and/or form

229 large macromolecular aggregates in pseudo-micellar fashion. In both cases,

230 polar functional groups are likely pointed to the external water phase, while the

231 lipophilic C moieties are held in the inner structural core. For their chemical

232 nature assessed by Table 1 data and their solution behavior indicated by Fig. 2,

233 the SBO used in this work qualified as dispersants in water phase capable to

234 interact with silica particles with their polar functional groups, to organize the

235 bonded silica particles around their pseudo-micellar structural assembly and to

236 allow, upon removal of the organic phase by calcinations, coalescence of the

237   pristine silica particles into a silica network following the shape of the organic

238   dispersant.

239   Figure 2 reports the water surface tension (γ) vs. SBO concentration (Cs).

240

241   *Physico-chemical characterization of silica prepared in the presence of SBO*

242   Under the experimental conditions of this work (see Experimental section) the

243   commercial silica powder was added to water containing SBO under stirring.

244   The resulting suspension was then allowed to thicken to a pellet which was

245   dried and calcined at 500°C to remove all organic material. This procedure has

246   been found to yield monolithic materials which are compact, assume the shape

247   of the container in which they are produced, can be handled without breaking or

248   disaggregating in powder form and maintain dimensional stability in water over

249   the 1-11 pH range. Figure 3 shows the images relative to the monolith

250   preparation steps into cylindrical shape by performing the above procedures in

251   a beaker: i.e. the black pellet formed by SiO_2 and SBO dried at room

252   temperature (left section) and the white material after calcination (right section).

253   Analyses carried out by transmission electron microscopy (TEM) showed

254   (Figure 4, left image) that the pristine silica powder is made up of small particles

255   of ~ 10 nm width or less, producing large interparticle void spaces, whereas the

256   monolith (Figure 4, right image) exhibits less and smaller interparticle void

257   spaces.

258   Gas-volumetric analysis of N_2 adsorbed at 77K confirmed that the monoliths

259   had pore sizes distribution peaking at smaller diameter levels than for the

260   powdery pristine silica material. For both powder and monolith silica, Figure 5

261 reports the adsorption isotherms (Figure 5 A) and the pore size distribution

262 (Figure 5 B) as obtained applying BJH model to the desorption experimental

263 data. Table 3 reports the relative specific surface area calculated via BET model

264 and the BJH-desorption total pore volume.

265 The adsorption-desorption isotherms (Figure 5 A) show hystheresis loops at

266 high values of relative pressure indicating the presence of large pores. The

267 extent of porosity changes passing from the powder to the monolith sample.

268 The BJH model applied to the isotherms desorption branch indicates that the

269 powder is macroporous and that the monolith formation occurs with reduction of

270 the pores width. Indeed, Figure 5 B shows that the pore size distribution peaks

271 at 400 Å for the powder and at 330 Å for the monolith. At the same time, Table

272 3 shows that the BET specific surface area and the total pore volume decrease

273 consistently (24% and 39% respectively) from the powder to the monolith.

274

275 *Composition and activity of silica-immobilized Soybean Peroxidase (SBP)*

276 *biocatalyst*

277 As described in more details in the Experimental section, SBP was immobilized

278 on both powder and monolith following a known procedure.[13] In this procedure,

279 the product of the reaction of silica and 3-aminopropyltriethoxysilane is first

280 obtained and then reacted with glutaraldehyde and SBP according to the

281 reaction scheme reported in Figure 6.

282 Table 4 reports the reaction yield of the immobilization process and the SBP

283 content in the final product for silica in powder and in monolith forms.

284 It may be observed that the SBP concentration in the powder is significantly

285 higher than in the monolith, and this seems consistent with the higher specific

286 surface area of the powder compared to the monolith.

287 The immobilized SBP on powder (P-SBP) and monolith silica (M-SBP) were

288 tested for their catalytic activity by the DMAB-MBTH reaction (exemplified in

289 Figure 7) in comparison with the same reaction performed with free SBP in

290 solution and in the absence of SBP.

291 The results are reported in Figure 8. As expected, the experimental data

292 demonstrate that the immobilized SBP allows a slower conversion of the

293 substrate to the reaction product. The initial reaction rate decreases in the order

294 free SBP > M-SBP > P-SBP > control. However, after two hours the M-SBP

295 catalyst allows to achieve the same 95% reagent conversion as free SBP in

296 solution, whereas the P-SBP catalyst is slower and less efficient. Furthermore,

297 P- SBP does not exceed 75% conversion of the reagent even after four hours of

298 reaction (data not shown). To test performance stability upon repeated recovery

299 and recycling, the immobilized catalysts were recovered from the reaction

300 medium after two hours, simply taking the M-SBP sample out from the reaction

301 mixture, or by filtration the suspension of P-SBP. Both samples were washed

302 with acetate buffer to remove product and reagents residues from the reaction

303 medium physically adsorbed on the catalyst, and used again to start a new

304 reaction with fresh reagents. This procedure was repeated twenty times. At

305 each cycle, the monolith immobilized catalyst (M-SBP) was easily removed from

306 the reaction medium by simply picking it out, whereas the powder had to be

307 filtered. Figure 9 reports the biocatalyst activity measured as % of retained

308 activity as function of the number of reaction cycles.

309 It may be observed that, after an initial activity decline, both the monolith and

310 the powder tend to remain at a constant value, at about 75-80% of the initial

311   activity. This appears slightly higher in the case of M-SBP.

312

313   ***Discussion***

314   It has been found in this work that the polymeric bio-organic substances (SBO)

315   isolated from urban vegetable refuse allow to fabricate a mesoporous silica

316   monolith (Figure 3) starting from commercial silica powder. Compared to the

317   powder, the silica monolith exhibits (Table 3 and Figures 4-5) lower specific

318   surface area, total pore volume and pore size, mostly concentrated at 330 Å

319   width. The pore size distribution peaking at 250-350 Å was observed also for

320   silica prepared by sol-gel reaction in the presence of a similar SBO material as

321   used in the present work.[3] This validates the expectation (see characterization

322   of SBO section) that, either in the sol-gel formation reaction and in the

323   dispersion of commercial silica, both carried out in the presence of SBO,

324   particles might form and/or coalesce into a silica network following the shape of

325   the organic polymeric substance. The quasi coincidence of the pore size

326   distribution peak of sol-gel and dispersed silica suggests that either SBO used

327   in the present work and the polymeric bio-organic substances used in previous

328   work,[3] although sourced from different biowastes, have the same behavior in

329   water solution and yield pseudo-micellar assemblies of similar size. The results

330   of this work obtained with commercial silica, therefore, and those of previous

331   work[3] obtained with sol-gel synthesized silica, confirm the property of polymeric

332   bio-organic substances isolated from urban bio-wastes to perform as templates

333   for the fabrication of mesoporous inorganic oxides. This property stems from

334   their solution behavior to form large pseudo-micelles either by their molecular

335   conformation and/or by intermolecular aggregation. With silica, the template

336 function seems effective either during sol-gel formation of silica and in the

337 process of dispersing preformed silica.

338   In the present work, the additional property of SBO to perform as binder for the

339 formation of silica monoliths has been evidenced. This is certainly due to the

340 presence of the inorganic residues (specifically SiO_2 and salts) which can act as

341 melting mixture.[14-16] In fact, the fabrication of the monolith fails in the presence

342 of ash-free SBO (i.e., SBO treated with HF in order to eliminate silica). In this

343 case only aggregated powder is obtained and no modifications of morphological

344 features is observed with respect to the original FK320 powder.

345 While monoliths formation, as exemplified in Figure 3, might propose the use of

346 SBO for the fabrication of porous ceramics and other materials in aqueous

347 media and using commercial preformed powdery particles, for heterogeneous

348 biocatalysis, specifically addressed in the present work, the use of a monolith-

349 like material, coupled to its mesoporosity features, is quite relevant for the

350 following reason. Recovery of the immobilized biocatalyst in monolith form from

351 the reaction medium is much easier and more efficient than in the case of the

352 powdery biocatalyst. The results in Figure 9 show that repeated recovery of the

353 monolith biocatalyst is possible with a limited activity loss occurring only in the

354 first three cycles and being inferior to the activity loss for the powdery

355 biocatalyst.

356   In addition to the improved performance upon being repeatedly cycled, the

357 monolith immobilized biocatalyst appears to exhibit higher kinetic activity

358 (Figure 8) than the powder immobilized biocatalyst, in spite of the fact that the

359 latter contains more SBP (Table 3). This suggests that, for the specific DMAB-

360 MBTH probe reaction used in this work, the morphological features of the

361 immobilized catalyst are more important than the amount of immobilized

362 catalyst. The higher performance of the monolith could be due to the presence

363 of mesopores where the active peroxidase is concentrated in confined spaces

364 yielding well -accessible micro-reactors and/or allowing better contact among

365 the reagents than in the case of the powder. These morphological features,

366 coupled to higher dimensional stability, may also be the reason of the higher

367 activity stability exhibited by the monolith compared to the powder catalyst when

368 recycled repeatedly. The results certainly encourage further studies on

369 polymeric organic substances isolated from different sources to establish

370 property-chemical nature-source relationships for the development of green

371 chemical technology.

372

379

380 **References**

381 [1] Montoneri E, Mainero D, Boffa V, Perrone DG, Montoneri C.

382   Biochemenergy: a project to turn a urban wastes treatment plant into

383   biorefinery for the production of energy, chemicals and consumer's products

384   with friendly enviromental impact. Int. J. Global Environmental Issues

385   2011;11:170-196, and references therein.

386   [2] Montoneri E, Boffa V, Savarino P, Perrone DG, Montoneri C, Mendichi R,

387   Acosta EJ, Kiran S. Behaviour and properties in aqueous solution of bio-

388   polymers isolated from urban refuse. Biomacromolecules 2010;11:3036-

389   3042.

390   [3] Boffa V, Perrone DG, Montoneri E, Magnacca G, Bertinetti L, Garlasco L,

391   Mendichi R. A waste derived biosurfactant for preparation of templated silica

392   powders. ChemSusChem 2010;3:445-452.

393   [4] Zhang Y, Hu L, Han J, Jiang Z, Zhou Y. Soluble starch scaffolds with

394   uniaxial aligned channel structure for in situ synthesis of hierarchically porous

395   silica ceramics. Microporous and Mesoporous Materials 2010;130:327–332.

396   [5] Geng Z, Rao KJ, Bassi AS, Gijzen M, Krishnamoorthy N. Investigation of

397   Biocatalytic Properties of Soybean Seed Hull Peroxidase. Catalysis today

398   2001;64:233-238.

399   [6] Marchis T, Avetta P, Bianco Prevot A, Fabbri D, Viscardi G, Laurenti E.

400   Oxidative degradation of Remazol Turquoise Blue G 133 by soybean

401   peroxidase. J. Inorg. Biochem. 2011;105:321-327.

402   [7] McEldoon JP, Dordick JS. Extraordinary Thermal Stability of Soybean

403   Peroxidase. Biotechnol Prog. 1996;12:555-558.

404   [8] Boscolo B, Laurenti E, Ghibaudi E. ESR Spectroscopy Investigation of the

405   Denaturation Process of Soybean Peroxidase Induced by Guanidine

406   Hydrochloride, DMSO or Heat. Protein J. 2006;25:379-390.

[9] Marchis T, Cerrato G, Magnacca, Crocellà V, Laurenti E. Immobilization of soybean peroxidase on aminopropyl glass beads: Structural and kinetic studies. Biochem. Eng. J. 2012;67:28-34.

[10] Brunauer S, Emmett PH, Teller E. Adsorption of gases in multimolecular layers. J.Am.Chem.Soc. 1938;60:309-319.

[11] Barrett EP, Joyner LG, Halenda PP. The Determination of Pore Volume and Area Distributions in Porous Substances. I. Computations from Nitrogen Isotherms. J.Am.Chem.Soc. 1951;73:373-380.

[12] Ngo TT, Lenhoff HM. A sensitive and versatile chromogenic assay for peroxidase and peroxidase-coupled reactions. Anal. Biochem. 1980;105:389-397.

[13] Weetall HH. Preparation of immobilized proteins covalently coupled through silane coupling agents to inorganic supports. Applied Biochemistry and Biotechnology 1993;41:157-187.

[14] Knechtel R. Glass frit bonding: an universal technology for wafer level encapsulation and packaging. Microsyst Technol. 2005;12:63-68.

[15] Sun Z, Pan D, Wei J, Wong CK. Ceramics bonding using solder glass frit. Journal of Electronic Materials 2004;33(12):1516-1523.

[16] Xu X, Zhuang H, Li W, Jiang G. Bonding behavior of copper thick films containing lead-free glass frit on aluminum nitride substrates. Ceramics International 2004;30:661-665.

[17] Montoneri, E., 2012. Biochemenergy, available at www.biochemenergy.it (accessed March 20, 2012).

Figure captions

432   Figure 1. Virtual molecular fragments for SBO isolated from UBW.

433   Figure 2. Surface tensione (γ) versus SBO concentration (Cs) in water.

434   Figure 3. Silica monolith after drying at room temperature (left image) and after

435   calcination at 500°C for 4 hours (right image).

436   Figure 4 - TEM image of the monolith (right section) compared to the powder

437   (left section).

438   Figure 5 - N_2 adsorption-desorption isotherms at 77K (left section A) and pore

439   size distribution calculated via BJH model on desorption data (right section B)

440   for silica powder (solid line, no symbols) and for silica monolith (line with triangle

441   symbols).

442   Figure 6. Reaction scheme for the immobilization of SBP on silica

443   Figure 7. Test reaction catalyzed by SBP in homogeneous solution or

444   immobilized on silica[12].

445   Figure 8. Conversion rate of the DMAB-MBTH reaction at 25 °C in the absence

446   (control) and presence of SBP, either free or immobilized on silica powder (P-

447   SBP) and monolith (M-SBP).

448   Figure 9. Kinetic tests of SBP immobilized on silica powder (P-SBP) and

449   monolith (M-SBP) for repeated reaction cycled. The activities were measured as

450   % decrease of absorbance at 590 nm after 120 min of reaction time.

451

Table 1. Content of C moieties and functional groups as C meq g^{-1} in SBO

Cal[a]	NR[b]	OR[b]	OCO	Ph[c]	PhOY[d]	PhOH	COOH	CON	C=O
11.7	2.32	4.20	0.13	4.26	0.52	1.64	3.84	0.45	1.49

[a]alipahtic C; [b]R = alkyl C; [c]Ph = aromatic C, except PhO C; [d]PhO = aromatic C bonded to O as in dyaryl ethers and alkyl aryl ethers according to Y = R, Ph.

Table 2. Percentages (w/w) of inorganic components and ash[1]

SiO$_2$	Fe$_2$O$_3$	Al$_2$O$_3$	MgO	CaCO$_3$	K$_2$CO$_3$	Na$_2$CO$_3$	Total	Ash[a]
5.45	1.10	0.93	1.87	15.16	6.34	0.37	31.2	27.9

[a]from residue after calcination at 650°C

Table 3 - Morphological data for silica powder and monolith

Sample	BET (m^{2}g^{-1})	Total Pore Volume (cm^{3}g^{-1})
powder	164	1.61
monolith	124	0.98

Table 4. Yield and product data for SBP immobilization reaction according to Figure 6.

Sample	% immobilization[a]	mg SBP/g sample
P-SBP[b]	81.2	15.6
M-SBP[c]	59.4	11.4

[a] The % immobilization was calculated as the difference between the initial amount of enzyme and that recovered in the washing liquid in respect to the initial amount of SBP. The concentration of SBP in solution was determined by measuring the absorbance at 403 nm; [b] powder immobilized SBP; [c] monolith immobilized SBP.
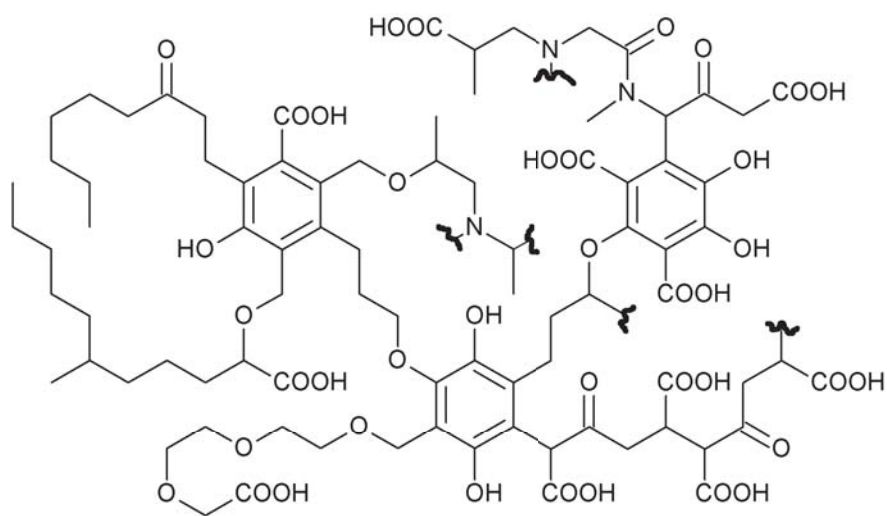
473

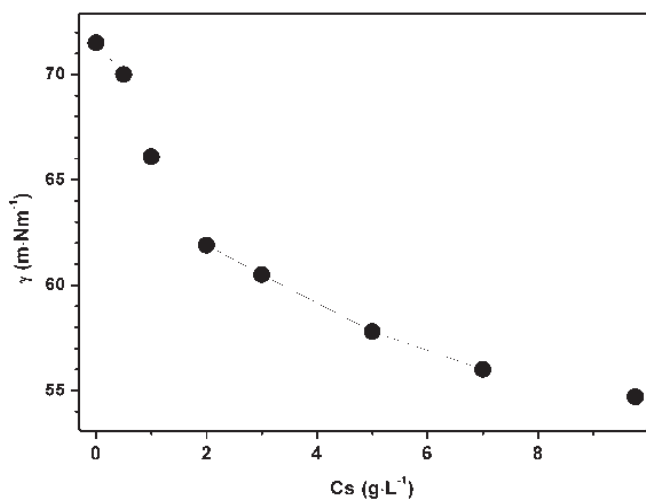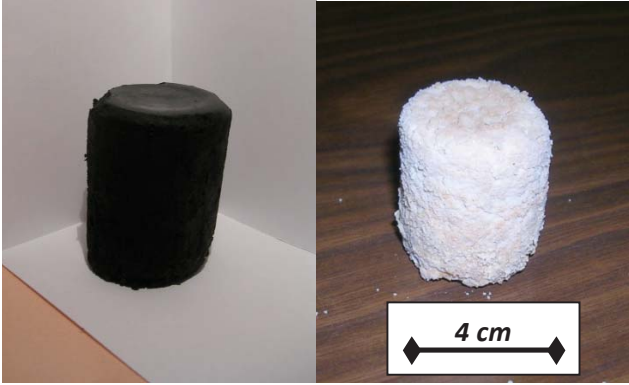474   Figure 1

475

476

477

478

479   Figure 2

480
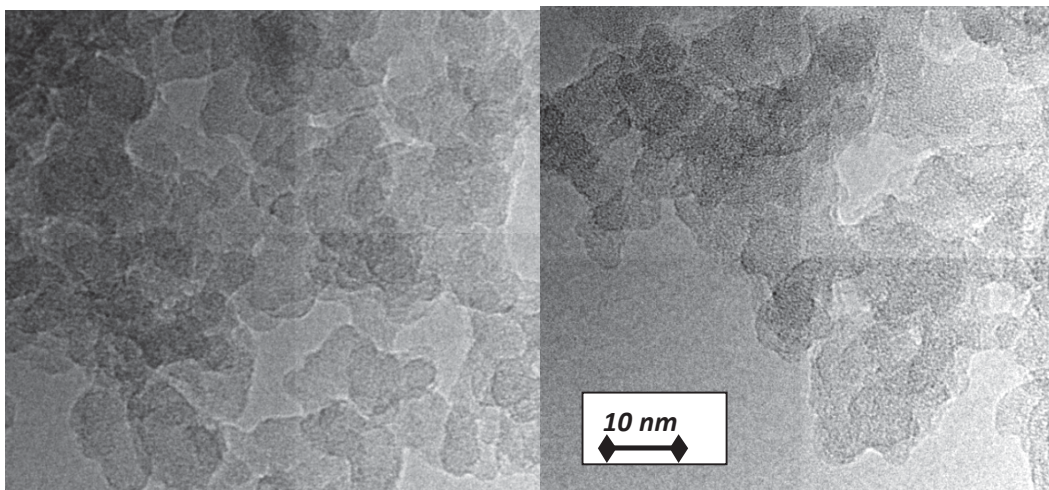481

482

483   Figure 3

484
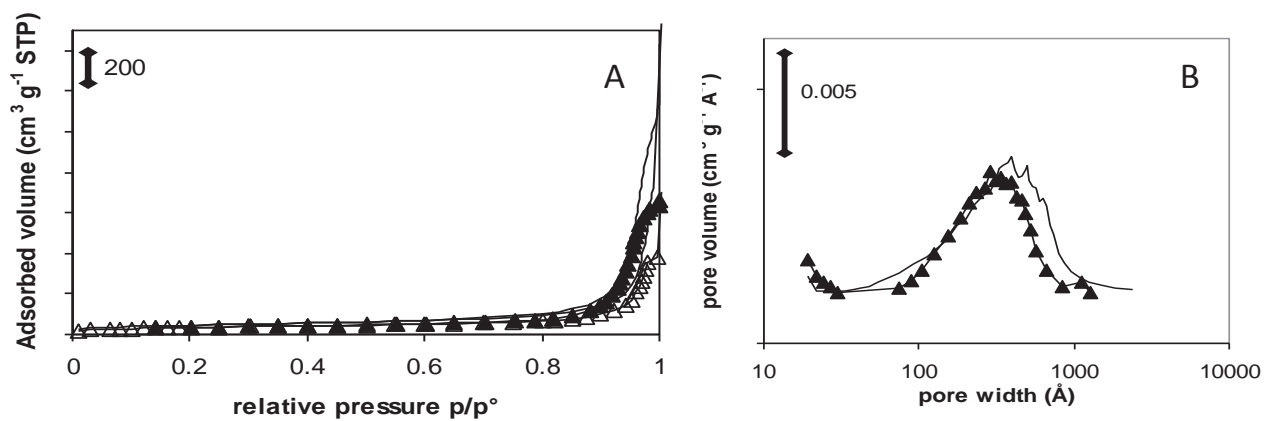
485

486

487   Figure 4

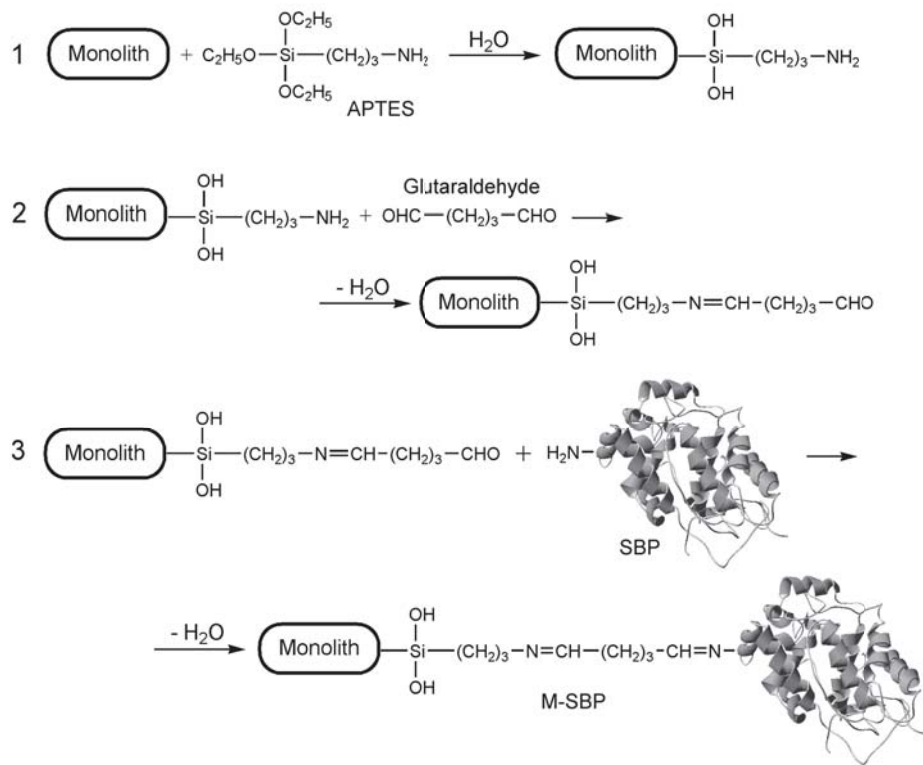

488
489
490

491   Figure 5
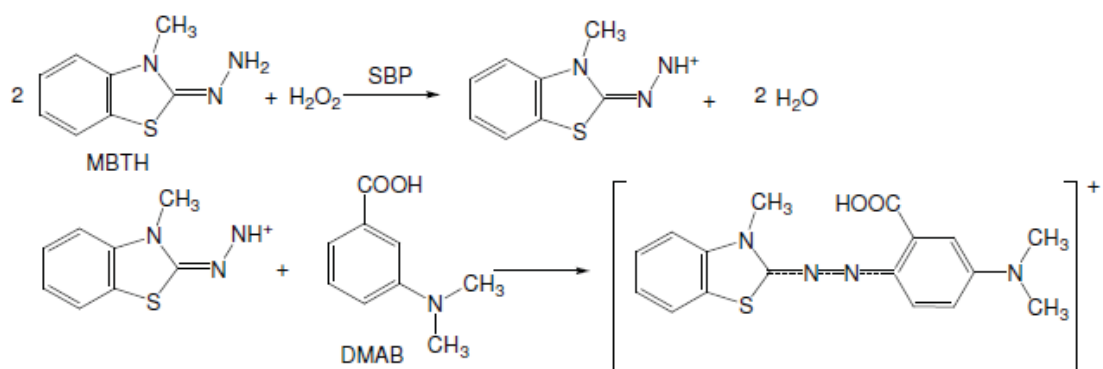

500

501

502   Figure 6
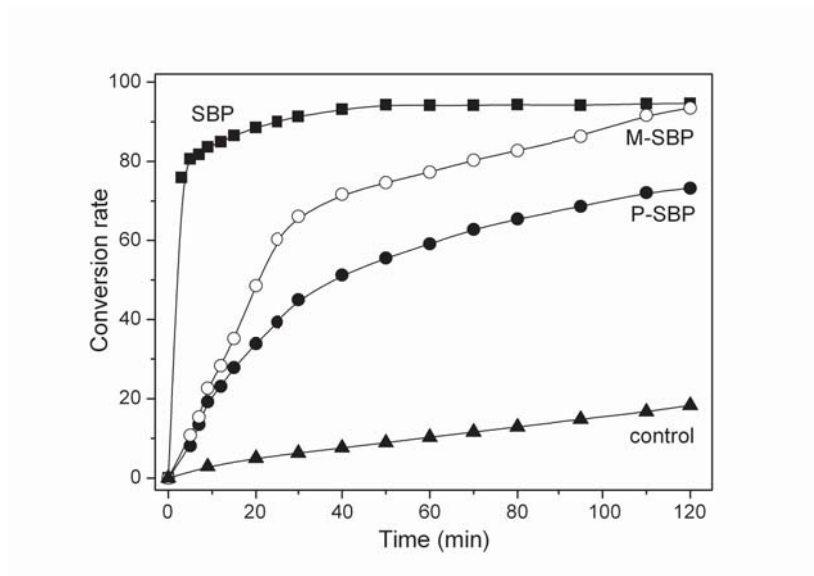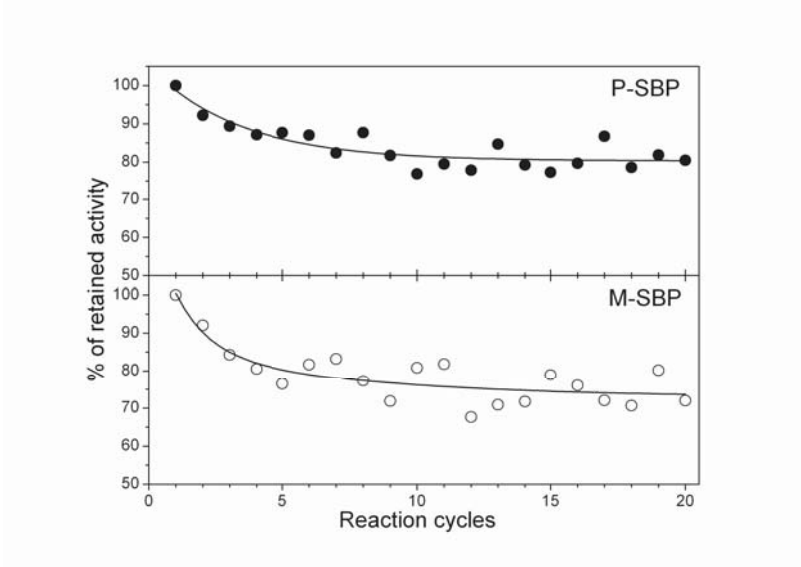

503
504

505

506   Figure 7

507

508

509

510   Figure 8

511
512
513

514   Figure 9

515

516

517